Fuzzy Logic Approach to Type-1 Diabetes Management (T1D): A Comparative Analysis of Open and Closed-loop Systems under a Four-day Meal Protocol

Isah Ndakara Abubakar[1], Moad Essabbar[2], Hajar Saikouk[3] and El Hilali Alaoui Ahmed[4]

[1.2.4]Euromed University of Fes, UEMF, Morocco
[3]Mohammed V University of Rabat, Morocco
[1]Federal University of Technology, Minna, Nigeria
Corresponding Author's E-mail: is.abubakar@ueuromed.org

Abstract: Efficient postprandial blood glucose control is imperative for the well-being among people experiencing diabetes. This study conducted a contrastive analysis between open and closed-loop systems, utilizing Hovorka's model to simulate the glucose-insulin physiological response over a four-day meal protocol. The closed-loop system incorporates a three-stage fuzzy logic control approach. Initially, a non-sequential model of the glucose-insulin monitoring mechanism was established. Subsequently, an iterative hierarchical framework was utilized to devise a propping control policy for insulin administration, incorporating inputs from two Mamdani Fuzzy Inference System (FIS) entities. Lastly, the control system was tuned by optimizing the fuzzy membership functions. The obtained results demonstrate superior glycemic conditions in the closed-loop scenario compared to the open-loop system across the four days, with improvements of 88.2% at the outset, 80.9% by the following day, 94.2% on the third day, and 92.6% on the fourth day.

Keywords: Closed-loop; diabetes; fuzzy logic controller; insulin; meal; open loop

1. Introduction

Diabetes is a persistent autoimmune illness marked by the pancreas's incapacity to generate insulin[1-7]. Maintaining precise blood glucose levels (BGLs) is paramount for individuals with T1D to prevent both short-term issues, such as hypo- or hyperglycemia, and long-term complications, such as renal failure, nerve damage, and cardiovascular disease [8-12]. The normal BGL, considered optimal, falls within 70 and 180 mg/dl [13]. Despite the importance of overall glycemic control, individuals with T1D encounter specific challenges during the postprandial period, when glucose levels tend to rise after meals. Postprandial hyperglycemia poses a risk of complications, increasing the overall glycemic load [14, 15]. The rapid absorption of carbohydrates, variations in digestion rates, and interaction of insulin kinetics with food intake make it challenging for traditional management techniques to exert precise control during this critical post-meal period [16, 17]. In the context of insulin infusion, diabetic individuals can opt for manual injection via a syringe or automated administration via an insulin pump [18, 19]. The manual injection is prone to errors, representing an open-loop scenario, whereas the insulin pump provides continuous subcutaneous insulin infusion in a closed-loop system. Addressing post-meal blood glucose regulation has been the focus of research, and various control architectures have been proposed. In [20], a framework was introduced to address blood glucose (BG) regulation in meal protocol with reduced CHO intake. Controller design was accomplished by applying a linear matrix inequality technique. Another study [21] developed a mechanism for creating a balance between hypo and hyperglycemic states. Additionally, a controller [22] based on the Mamdani-type fuzzy scheme was suggested to supervise blood glucose levels. Utilizing the Grey Wolf optimization technique, researchers [23] designed a type 2 fuzzy controller for stabilizing blood glucose using the Bergman minimal model for glucose-insulin kinetics. Furthermore, [24] explored four different optimization methods to fine-tune the uncertainty footprint of the controller, aiming to select the most effective control approach for regulating blood glucose levels in a nonlinear model of T1D. While existing studies have addressed blood

Received: May 7th, 2024. Accepted: June 11th, 2025
DOI: 10.15676/ijeei.2025.17.2.11

glucose levels after meal consumption, there remains a gap in achieving optimal insulin infusion alongside optimal blood glucose levels. Therefore, it is crucial to develop an approach to solve this challenge. This research demonstrates a fuzzy logic technique to address the optimization of blood glucose levels and insulin infusion. The approach involves a comparative analysis between open- and closed-loop mechanisms that allow individuals with the disease. This analysis is conducted within the context of a four-day meal protocol, utilizing Hovorka's model. In summary, this research study provides significant contributions to the field and can be outlined as follows:

- The detailed results in Section 4 reveal a glycemic state achievement of 88.2% at the outset, 80.9% by the following day, 94.2% on the third day, and 92.6% on the fourth day.
- We employed an iterative hierarchical framework to devise a propping control policy for insulin administration. This involved the use of two Mamdani (FIS) to enhance the precision of insulin infusion control.
- The Hovorka scheme was utilized in this study to determine variables, allowing for the consideration of diverse profiles of patients with diabetes. This model enhances the understanding of system dynamics and aids in tailoring the proposed controller to different patient attributes.

The subsequent sections of this paper follow a systematic organization. Section 2 outlines the adopted methods, while Section 3 offers an overview of the results. A detailed discussion of evaluation metrics is depicted by Section 4, lastly, discussion and conclusion in Section 5.

2. Materials and Methods

The methodology section comprises several key components, as delineated by the following subheadings:

A.1. The intricate structure of (T1DM) attributed to nonlinearity

The intricate dynamics of T1D, represented by the Hovorka model [25], demonstrate its nonlinear nature influenced by biological factors impacting BGL. Understanding these complexities is vital for developing effective treatment strategies and improving outcomes in diabetes care.

A.2. Hovorka framework

The framework is scheduled into three (3) segments: a glucose component managing glucose uptake, delivery, and elimination; an insulin subsystem overseeing insulin absorption, distribution, and disposal; and an insulin action segment regulating insulin's effects on delivery, elimination, and external extraction.

- In this study, the glucose segment played a central role and incorporated several key components. It notably includes a representation of heart function, detailed through a series of segmental equations, specified as equations (1) and (2), which describe glucose dynamics. Additionally, the subsystem features a model illustrating the gut's glucose absorption rate, captured in (3).

$$\frac{DQ_1(t)}{D_{(t)}} = -\left[\frac{F_{01}c}{V_G G(t)} + X_1(t)\right] Q_1(t) + k_{12}Q_2(t) - F_R + U_G(t) + EGP_0[1 - X_3(t)]\# \quad (1)$$

$$\frac{DQ_2(t)}{D_{(t)}} = X_1(t)Q_1(t) - [k_{12} + \mathrm{X}_2(t)]Q_2(t)y(t)G(t) = Q_1(t)/V_G \quad (2)$$

$$U_G(t) = \frac{D_G A_G t e^{-t/t_{maxG}}}{t^2{}_{maxG}} \quad (3)$$

Given that Q_1 and Q_2 indicate quantities of glucose in the reachable and no-reachable portion, k_{12} signifies the transition pace value from the reachable and no-reachable portion; V_G stands for dispersion volume of the reachable portion; y and G denote glucose concentrations; and EGP_0 hypothesizes zero endogenous glucose production. Additionally, $F_{01}c$ denotes total glucose flow independent of insulin designated to external glucose rates, F_R signifies renal

glucose elimination more than the specified limit, U_G symbolizes the gut intake rate, t_{maxG} indicates the period when glucose reaches its peak concentration in the accessible glucose area, D_G relates to the quantity of CHO metabolized, and A_G represents the CHO effectiveness. It is important to note that

$F_{01}c$ = Overall glucose flux independent of insulin, represented as

$$F_{01}c = \begin{cases} F_{01}, & if\ G \geq 4.5mmol/L \\ F_{01}, & G/4.5\ Otherwise \end{cases}$$

F_R = Renal glucose removal more than the specified limit of 9 mmol/L, expressed as

$$F_R = \begin{cases} 0.003(G-9)V_G, & if\ G \geq 9mmol/L \\ 0, & Otherwise \end{cases}$$

- In the insulin section, the mechanism of insulin absorption is distinctly elucidated by equations (4) and (5), while (6) delineates the plasma density of insulin. This segment offers a thorough examination of the management and measurement of insulin levels within the network.

$$\frac{DS_1(t)}{D_{(t)}} = u(t) - \frac{S_1(t)}{t_{maxI}} \quad (4)$$

$$\frac{DS_2(t)}{D_{(t)}} = \frac{S_1(t)}{t_{maxI}} - \frac{S_2(t)}{t_{maxI}} \quad (5)$$

$$\frac{DI(t)}{D_{(t)}} = \frac{U_I(t)}{V_1} - k_e\, I(t) \quad (6)$$

where S_1 and S_2 denote the digestion of underneath offered short-acting insulin, u(t) signifies insulin administration, and t_{maxI} indicates the time required for peak insulin digestion. The pace of insulin absorption was calculated using $U_I = S_2(t)/t_{maxI}$. Additionally, k_e denotes the proportion of clearance and V_I is the insulin diffusion volume.

- In the part discussing insulin's influence, it's highlighted that the subsystem incorporates three specific impacts of insulin on glucose dynamics, detailed (7), (8), and (9). Additionally, insulin absorption rates in both slow and fast channels is depicted by (10), (11), (12), and (13).

$$\frac{Dx_1}{D_{(t)}} = -k_{a1}\, x_1(t) + k_{b1}\, I(t) \quad (7)$$

$$\frac{Dx_2}{D_{(t)}} = -k_{a2}\, x_2(t) + k_{b2}\, I(t) \quad (8)$$

$$\frac{Dx_3}{D_{(t)}} = -k_{a3}\, x_3(t) + k_{b3}\, I(t) \quad (9)$$

$$\frac{DQ1_a}{D_{(t)}} = ku\ - k_{a1}\, Q_{1a}\ - \mathrm{L}D_a \quad (10)$$

$$\frac{DQ1_b}{D_{(t)}} = (1-k)u\ - k_{a2}\, Q_{1b}\ - LD_b \quad (11)$$

$$\frac{DQ_2}{D_{(t)}} = k_{a1}\, Q_{1a}\ - k_{a1}\, Q_2 \quad (12)$$

$$\frac{DQ_3}{D_{(t)}} = k_{a1}\, Q_2\ + k_{a2}\, Q_{1b}\ - k_e\, Q_3 \quad (13)$$

In the sense that X_1, X_2, and X_3 defines the impact of insulin on glucose digestion, glucose elimination, and egp, k_{a1}, k_{a2}, and k_{a3} represent deactivation rates; and k_{b1}, k_{b2} and k_{b3} symbolize activation rates. Moreover, u denotes the insulin input, Q_{1a} and Q_{1b} indicate the amount of insulin in the slower absorption pathway comprising two compartments, Q_2 represents the quantity of insulin in the rapid absorption area, V denotes the insulin distribution volume, k represents the portion of the complete input flow allocated to the gradual absorption area, k_e represent the proportion of clearance, and LD_a and LD_b are the rate of insulin breakdown at the infusion site. Equations (14) and (15) portray the Michaelis-Menten kinetics for LD_a and LD_b.

$$LD_a = V_{max,LD}\, Q_{1a} / \left(\mathrm{K}_{\mathrm{M,LD}}\ + Q_{1a}\right) \quad (14)$$

$$LD_b = V_{max,LD}\, Q_{1b} / \left(\mathrm{K}_{\mathrm{M,LD}}\ + Q_{1b}\right) \quad (15)$$

$V_{max,LD}$ represent the point of permeation, and $K_{M,LD}$ indicate the insulin amount such that insulin degradation is comparable to fifty percent the peak level. Additionally, the coupled

ordinary differential equations (ODEs) in the Hovorka model were solved using the Runge-Kutta method, chosen for its accuracy and stability. Specifically, the fourth-order Runge-Kutta method (RK4) was selected due to its optimal balance between computational efficiency and precision, allowing for an accurate representation of the glucose-insulin dynamics over time. This method was implemented in MATLAB, which offers robust functions for solving systems of differential equations. Additionally, a convergence analysis was performed by varying the step size to ensure that the numerical solutions remained consistent, thereby validating the results.

A.2.1. Hovorka Model Assumptions

A.2.1.1. Insulin Absorption Submodel

- *Assumption 1*: The insulin absorption rate follows a biphasic profile, with an initial rapid absorption phase followed by a slower phase. This is based on the physiological observation of subcutaneous insulin kinetics.
- *Assumption 2*: The model assumes a uniform distribution of insulin in the subcutaneous tissue and neglects any variability in absorption due to site differences or individual patient factors.
- *Assumption 3*: Insulin degradation in subcutaneous tissue is not explicitly modeled and is considered negligible over the short-term simulation period

A.2.1.2. Glucose Kinetics Submodel

- *Assumption 1*: The glucose distribution between the plasma and interstitial compartments is assumed to be instantaneous and homogeneous, implying no time delay between changes in plasma glucose and interstitial glucose levels.
- *Assumption 2*: Glucose uptake by tissues (other than insulin-sensitive tissues) and glucose production are assumed to be constant and independent of insulin action, which simplifies the model by reducing the number of dynamic variables.
- *Assumption 3*: Renal glucose excretion occurs only when blood glucose levels exceed a specific threshold, reflecting the renal threshold for glucose reabsorption.

A.2.1.3. Insulin Action Submodel

- *Assumption 1:* The effect of insulin on glucose uptake and production is modeled as a time-delayed response, representing the physiological delay in insulin action on hepatic and peripheral tissues.
- *Assumption 2:* Insulin sensitivity is considered constant during the simulation period, assuming no acute changes due to meal.
- *Assumption 3:* The submodel assumes that the maximum effect of insulin on glucose production suppression and glucose uptake stimulation is bounded and reaches saturation at high insulin concentrations.

A.3. Nominal parameters, constants, and definitions in Hovorka's model

To simplify the model and ensure an accurate representation of the varied changes in BGL in patients with the condition during normal bodily functions, the model quantities were classified into parameters and constants. The values for these parameters and constants in the diabetic patient scheme were sourced from [25], and Tables 1 and 2 present the adopted values. *Furthermore,* the initial conditions and parameter values presented in Tables 1 and 2 were selected based on three key considerations [25-31]:

- *Alignment with the Hovorka Model:* The parameters are directly derived from the Hovorka model, a well-established framework for simulating glucose-insulin dynamics in type 1 diabetes patients. This model is widely recognized for its effectiveness in predicting blood glucose levels, and its parameters are thoroughly documented in the literature.
- *Evidence from Literature and Empirical Data:* The chosen parameter values are grounded in empirical data and have been validated by previous research studies, ensuring their reliability and accuracy.

- *Physiological Relevance:* Certain parameters were chosen to represent typical physiological conditions found in adolescent diabetes patients. This was done to ensure the study accurately reflects realistic scenarios.

These considerations ensure that the parameters used are both scientifically sound and applicable to the target population.

Table 1. The model constants

Abbreviation	Description	Amount	Unit
k_{12}	Transmission rate	0.6×10^{-2}	Min^{-1}
k_{a1}	Inactivation rate	0.6×10^{-2}	Min^{-1}
k_{a2}	Inactivation rate	0.6×10^{-2}	Min^{-1}
k_{a3}	Inactivation rate	0.3×10^{-1}	Min^{-1}
k_e	proportion of clearance	1.38×10^{-1}	Min^{-1}
V_I	Insulin diffusion volume	1.2×10^{-1}	Lkg^{-1}
V_G	Glucose dispersion volume	1.6×10^{-1}	Lkg^{-1}
A_G	CHO effectiveness	8×10^{-1}	unitless
t_{maxG}	Time-to-max CHO intake	4×10^{1}	Min

Table 2. The model parameters

Abbreviation	Description	Amount	Unit
$S_{IT}f=\frac{k_{b1}}{k_{a1}}$	Insulin susceptibility to delivery	5.12×10^{-2}	Min^{-1} per mU L^{-1}
$S_{ID}f=\frac{k_{b2}}{k_{a2}}$	Insulin susceptibility to elimination	8.2×10^{-3}	Min^{-1} per mU L^{-1}
$S_{IE}f=\frac{k_{b3}}{k_{a3}}$	Insulin susceptibility of egp	520×10^{-4}	Min^{-1} per mU L^{-1}
EGP0	EGP assumed to be unaffected by insulin	1.61×10^{-2}	mmol kg^{-1} min^{-1}
$F_{01}c$	Glucose flux not dependent on insulin	9.7×10^{-3}	mmol kg^{-1} min^{-1}
Q_{1a} , Q_{1b}	Slow chamber transfer rate	1.12×10^{-2}	sec^{-1}
Q2	Rapid chamber transfer rate	2.10×10^{-2}	sec^{-1}
$V_{max,LD}$	Point of permeation	1.93×10^{0}	mU/sec
k	Percentage in slow bandwidth	6.7×10^{-1}	unitless
$t_{max,I}$	Time until peak of short-acting insulin	55×10^{0}	Min

A.4. Utilizing Bayesian technique for estimating parameters

In the adopted model used in this study, the introduction of insulin induces nonlinearity, affecting several factors associated with glucose production, circulation, and elimination. Bayesian estimation of parameters, a scheme for determining parameters that vary over time, was employed to address the challenges associated with identifiability after estimation. Specifically, a multiple log-normal circulation for variables $S_{IT}f$, $S_{ID}f$, $S_{IE}f$, F_{01} and EGP_0, was established [25]. For practical execution and numerical consistency throughout improvement, this delivery was depicted as a uniform addition of 5 individual one-dimensional typical deliveries, each illustrated by an average of null and a standard deviation of one (pi ~ N(0, 1), i = 1,2,3,4, and 5), as represented in equations (16)–(20). The stochastic transformation scheme was applied to determine indices a_{ij} and b_i. Furthermore, the log-normal preexisting dispersion for the residual variable $t_{max,I}$ was adopted out of the study [25], standardized for numerical stability, and streamlined for implementation.

$$lnS_{IT}f = a11p1 + b1 \quad (16)$$

$$lnS_{ID}f = a12p1 + a22p2 + b2 \quad (17)$$

$$lnS_{IE}f = a13p1 + a23p2 + a33p3 + b3 \quad (18)$$

$$lnF01 = a14p1 + a24p2 + a34p3 + a44p4 + b4 \quad (19)$$

$$lnEGP0 = a15p1 + a25p2 + a35p3 + a45p4 + a55p5 + b5 \quad (20)$$

A.5. Component Interaction sand Integration in Model Components (A2, A3, and A4)

Part A2 lays the groundwork for the model by defining the glucose-insulin dynamics using the Hovorka framework, which consists of a set of ordinary differential equations (ODEs) that capture the interactions between insulin and glucose in the body. These equations are essential for accurately simulating the physiological processes that the model seeks to replicate. In Part A3, the model's necessary parameters, constants, and definitions are introduced. These include crucial elements such as glucose effectiveness, insulin sensitivity, and other physiological constants, which are vital for accurately representing the dynamics described in the Hovorka framework. Without these parameters, the model would lack the precision needed to effectively simulate real-world glucose-insulin interactions. Part A4 builds on the framework and parameters established in A2 and A3 by incorporating a Bayesian technique to refine these parameters. This approach is particularly beneficial for integrating prior knowledge and addressing uncertainties in the parameter estimation process, leading to more robust and personalized simulations. This refinement is essential for adjusting the nominal parameters to reflect individual patient variability, thereby enhancing the model's predictive accuracy.

The interaction among these components is as follows: The Hovorka framework (A2) provides the structural foundation, where the glucose-insulin dynamics are mathematically represented. The parameters and constants from A3 are integrated into this framework to ensure the model reflects typical physiological conditions. The Bayesian technique in A4 then refines these parameters based on observed data, allowing for personalization and improved accuracy. Together, these elements create a cohesive and dynamic model capable of simulating glucose-insulin interactions and adapting to patient-specific data.

A.6. Equilibrium points and linearized stability evaluation of Hovorka's model

The distinctive equilibrium points of the model, represented by (Q∗, I∗), are found by solving the equations dG/dt = 0 and dI/dt = 0. However, deriving explicit solutions for Q and I within the Hovorka model is challenging [25]. To evaluate the stability of the nonlinear model at the equilibrium points (Q, I), we applied the linearization method using the Jacobian matrix.

k_{12} = 0.006 Min^{-1}; k_{a1} = 0.006 Min^{-1}, k_{a2} = 0.006 Min^{-1}; k_{a3} = 0.003 Min^{-1}, k_e = 0.138 Min^{-1}; $S_{IT}f = \frac{k_{b1}}{k_{a1}}$ = 0.0512 min^{-1} per mUL^{-1} $S_{ID}f = \frac{k_{b2}}{k_{a2}}$ = 0.0082 min^{-1} per mUL^{-1}.

By linearizing the glucose dynamics for the first segment, we obtain (21):

Therefore, when linearizing the dynamics of glucose, particularly focusing on the first compartment, the resulting expression is as follows:

$$\frac{\delta Q_1(t)}{\delta_{(t)}} = -\left[\frac{F_{01}c}{V_G G(t)} + x_1(t)\right]\delta Q_1(t) + k_{12}\delta Q_2(t) - \delta F_R + \delta U_G(t) + \delta EGP_0[1 - x_3(t)] \quad (21)$$

Moreover, linearization of the second segment yields (22).

$$\frac{\delta Q_2(t)}{\delta_{(t)}} = \delta x_1(t)Q_1(t) - [k_{12} + x_2(t)]\delta Q_2(t)y(t)G(t) = Q_1(t)/V_G \quad (22)$$

where$\delta Q_1(t) = Q_1(t) - \mathrm{Q}*$ indicates the variation of glucose from its steady state. Essentially, the kinematic parameter of glucose is [K_{12} Q_2]. Additionally, linearization of the insulin dynamics results in (23).

$$\frac{\delta \mathrm{I}(t)}{\delta_{(t)}} = \frac{\delta U_I(t)}{\delta V_1} - \delta k_e\, I(t) \quad (23)$$

where $\delta I(t) = I(t) - I*$ indicates the variation of insulin from its equilibrium point, $\delta U_I(t)$ indicates the variation in external control, and δV_1 denotes the variation in the insulin distribution volume. The eigenvalues of the Jacobian matrix (J) for the linearized system were subsequently computed. Expressed as:

$$\mathrm{J}=\begin{bmatrix} -K_{12} & Q_2 \\ V_I & -K_e \end{bmatrix} = \begin{bmatrix} -0.006 & 0.021 \\ 0.12 & -0.138 \end{bmatrix}$$

Utilizing the notion of characteristic equations leads to the expression:

$$\text{So;}\begin{bmatrix} -0.006 - \lambda & 0.021 \\ 0.12 & -0.138 - \lambda \end{bmatrix}$$

$$\lambda^2 + 0.144\lambda + 0.003348 = 0$$

Hence, the solutions to the quadratic equation are:

$$\lambda = -0.072 \; ; \; \lambda = -0.216$$

Since eigenvalues exhibit negative real parts, the network achieves asymptotic stability, indicating a return to equilibrium. Consequently, according to the stability metrics, there is no requirement to augment the insulin treatment protocol as stable and effective glucose control has been achieved.

B. Proposed fuzzy logic controller architecture

The proposed framework, based on the FIS, introduces a robust system featuring two input and one output linguistic states. This design aims to effectively monitor BGL in individuals with diabetes by incorporating dynamic parameters. The two input linguistic variables, current glucose level (g(t)) and its rate of change (dg/dt), play a crucial role in quantifying real-time glucose dynamics. The output linguistic variable corresponds to the calculated insulin dosage, critical for maintaining glucose homeostasis. Using fuzzy logic principles, the controller defines fuzzy sets and determines membership function (MF) for input and output parameters. Triangular MF, known for their simplicity and efficiency, are utilized in this FLC. Figure 1 illustrates the MFs of the input variables. The FLC operates on a set of 27 IF-THEN rules, designed to introduce a relationship between target and real glucose values. These rules, formulated with minimum-type antecedents, optimize controller performance and minimize discrepancies. The rule base intricately links input and output membership functions, enhancing control capabilities. For precise control actions, the CENTROID defuzzification scheme aligns output decisions with desired control objectives. To improve effectiveness, a FIS tree control mechanism is proposed. Two Mamdani FISs are created using an incremental design strategy instead of a single FIS with 27 rules. The first-tier FIS pre-computes insulin infusion rates by aggregating BGL and rate (BGR) inputs. The second-tier addresses BGL acceleration to mitigate output noise, characterizing inputs with three MF each and five distinct membership functions for output representing various insulin dosages. Fuzzy rules in Tables 3 and 4, alongside Figure 2 depicting control operations, illustrate decision-making processes. Membership function parameters undergo tuning using the "tunefis" function to optimize controller performance. The controller integrates sensor-derived glucose information, including rate of change and acceleration, to calculate insulin infusion rates, as detailed in Table 5. Controller effectiveness is evaluated by comparing results across four days of meal protocols in open and closed-loop scenarios (Table 6). This comprehensive controller framework significantly enhances glycemic control in individuals with T1DM, providing improved accuracy and adaptability in managing BGL. Additionally, applying fuzzy logic in this methodology involves fine-tuning insulin administration based on heuristic rules that emulate the decision-making process of diabetes professionals. It's also important to note that the fuzzy logic system is integrated into the Hovorka model, which comprises coupled ordinary differential equations (ODEs) that represent glucose-insulin dynamics.

- *Integration of Fuzzy Logic with the Hovorka Model:* The Hovorka model captures the physiological interactions between glucose and insulin through its differential equations. Fuzzy logic is not directly used to solve these ODEs; instead, it is employed to enhance decision-making for insulin dosing based on the model's outputs.
- *Fuzzy Logic Control for Insulin Dosing:* The outputs of the Hovorka model, such as glucose concentration and insulin levels, are used as input variables for the fuzzy logic controller. This system utilizes a set of predefined fuzzy rules to assess these inputs and determine the optimal insulin dose. This approach is particularly effective for managing uncertainties and nonlinearities in glucose regulation.
- *Coupling Fuzzy Logic with Numerical Solutions:* The differential equations of the Hovorka model are numerically solved using the Runge-Kutta method. The resulting predicted blood glucose levels are then processed by the fuzzy logic controller, which dynamically adjusts

insulin delivery to maintain glucose levels within a target range. This integration enables the model to more accurately reflect real-world physiological responses.

In essence by combining the deterministic nature of the glucose-insulin dynamic model with the adaptive and rule-based decision-making capabilities of fuzzy logic, a robust control mechanism is created that can effectively handle patient-specific variations and uncertainties.

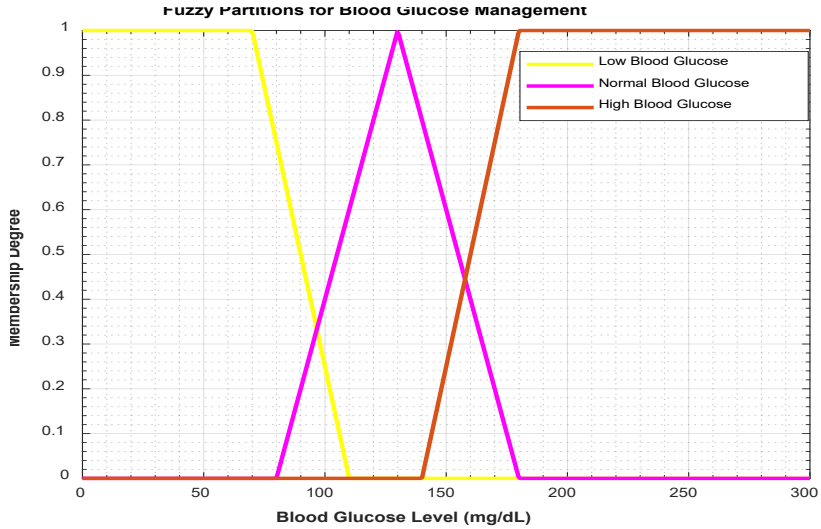

Figure 1. Membership function of input variables.

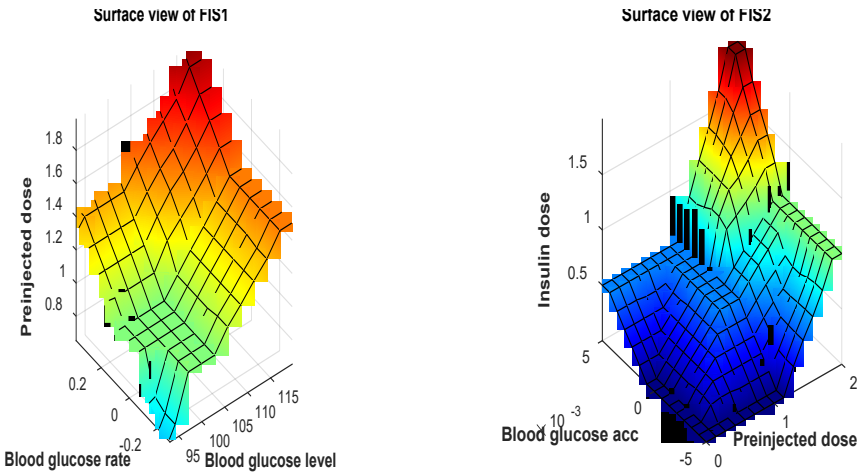

(**a**) (**b**)

Figure 2**.** Control operation surface representation (**a**) Graphical representation of the surface view of (FIS1) (**b**) Graphical representation of the surface view of (FIS2).

Table 3**.** Rule base of FIS1

	Blood glucose rate: N	Blood glucose rate: Z	Blood glucose rate: P
Blood glucose level: Low	Preinjected dose: Very High	Preinjected dose: Medium	Preinjected dose: Medium
Blood glucose level: Medium	Preinjected dose: Very Low	Preinjected dose: Medium	Preinjected dose: High
Blood glucose level: High	Preinjected dose: Medium	Preinjected dose: High	Preinjected dose: Very Low

Table 4. Rule base of FIS2

	Blood glucose acc: N	Blood glucose acc: Z	Blood glucose acc: P
Preinjected dose: Low	Insulin dose: Very High	Insulin dose: Very Low	Insulin dose: High
Preinjected dose: Medium	Insulin dose: Very Low	Insulin dose: Low	Insulin dose: Low
Preinjected dose: High	Insulin dose: Low	Insulin dose: Very Low	Insulin dose: Very Low

Table 5. Rule base of FIS2

	Blood glucose rate	N			Z			P		
	Blood glucose Acc	N	Z	P	N	Z	P	N	Z	P
Glucose Level	VH	2.00	1.80	1.60	1.50	1.30	1.20	1.40	1.70	1.10
	H	1.10	1.20	1.50	1.80	1.90	1.05	1.00	1.95	1.65
	M	0.50	0.60	0.80	0.90	1.00	0.40	0.30	0.25	0.00
	VL	0.40	0.30	0.20	0.50	0.60	0.70	0.15	0.10	0.08
	L	0.00	0.00	0.00	0.00	0.00	0.00	0.01	0.02	0.03

C. Four-Day Meal Protocol and Hovorka's Model Dynamics Representation

In this study, the four-day meal protocol, as outlined in [21], was employed alongside Hovorka's model [25] to capture the intricate glucose-insulin dynamics, providing a comprehensive representation of diabetic physiology. The meal protocol for each day is as follows:

C.1. Day 1

Breakfast at 8:00, consisting of 50g of Carbohydrates (CHO)
Lunch at 13:00, comprising 70g of CHO
Dinner at 20:00, with a CHO portion size of 65g

C.2. Day 2

Breakfast at 8:00, consisting of 60g of Carbohydrates (CHO)
Lunch at 13:00, comprising 90g of CHO
Dinner at 20:00, with a CHO portion size of 80g

C.3. Day 3

Three Meals and Three Snacks
8:00: 45g of CHO
10:00: 35g of CHO
14:00: 60g of CHO
17:00: 40g of CHO
20:00: 50g of CHO
23:00: 30g of CHO

C.4. Day 4

Two Meals
8:00: 50g of CHO
20:00: 80g of CHO

This designed meal protocol presented in C1-C4 is integral to the exploration of glucose-insulin dynamics and their response to varying carbohydrate intake. The utilization of Hovorka's model ensures a robust representation of diabetic physiology, allowing for a nuanced examination of the behavior of the system across different meal protocols. Figures 3–6 illustrate the dynamic relationship between glucose utilization and carbohydrate (CHO) intake over time across the four days. These visualizations served as crucial components in our analysis, offering insights into the temporal patterns of glucose utilization and CHO intake throughout the study duration.

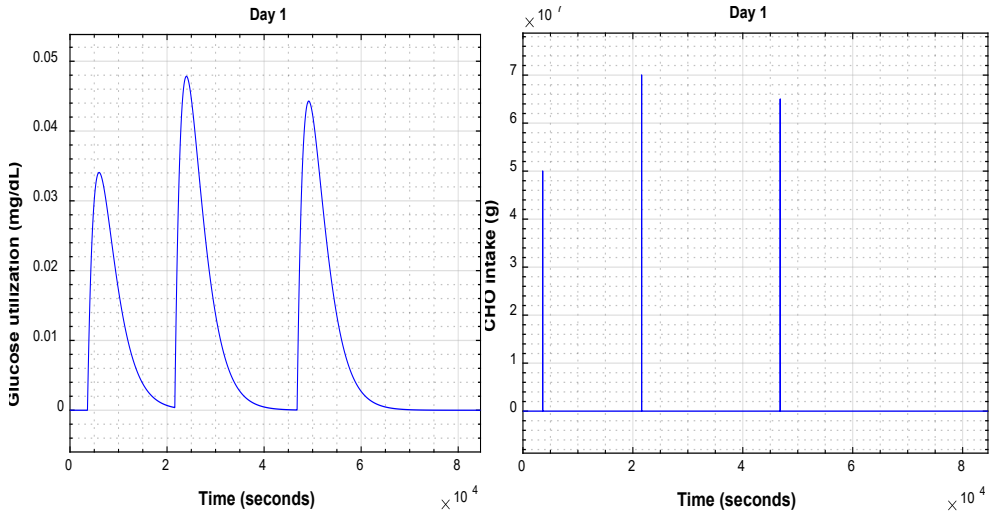

(a) (b)

Figure 3**.** Day 1. (**a**) Plot of glucose utilization against time (**b**) Plot of CHO intake against time

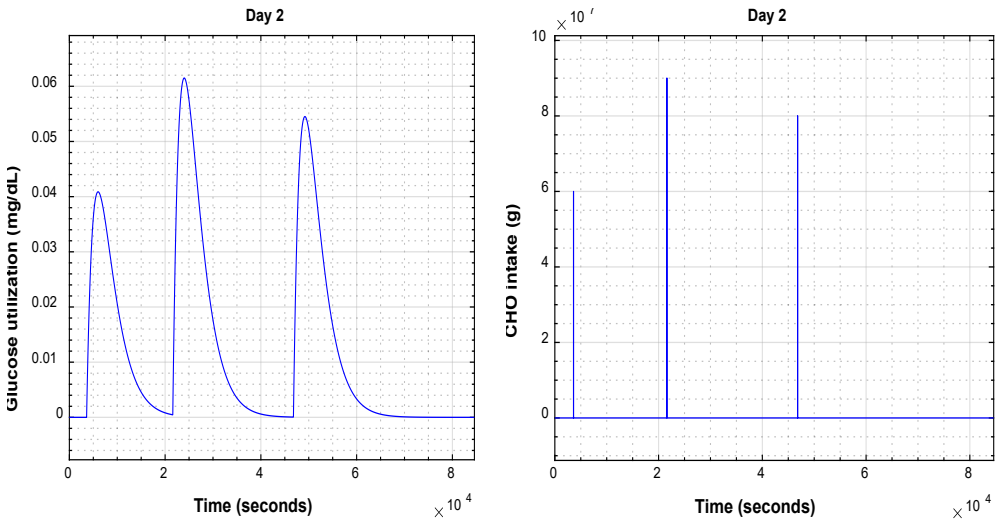

(a) (b)

Figure 4. Day 2. (a) Plot of glucose utilization against time (b) Plot of CHO intake against time

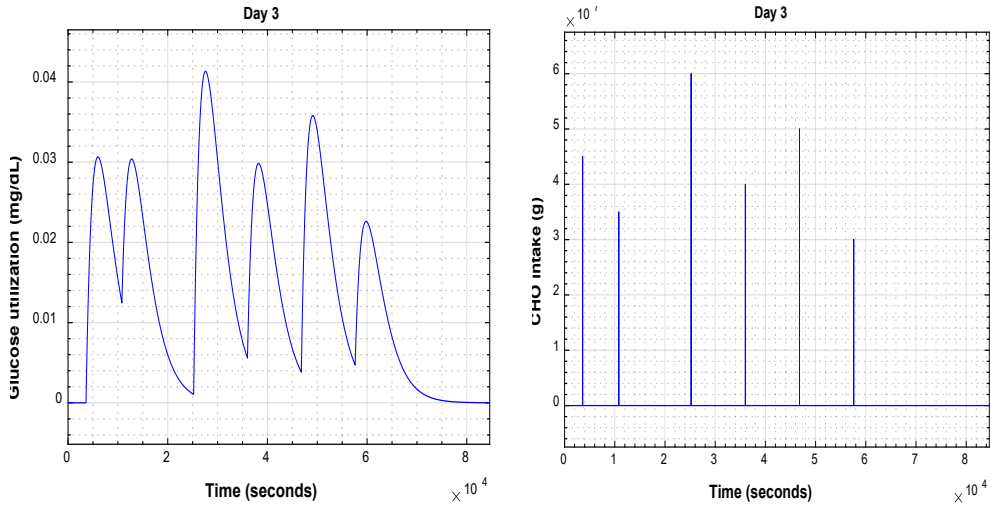

(**a**) (**b**)

Figure 5**.** Day 3. (**a**) Plot of glucose utilization against time (**b**) Plot of CHO intake against time

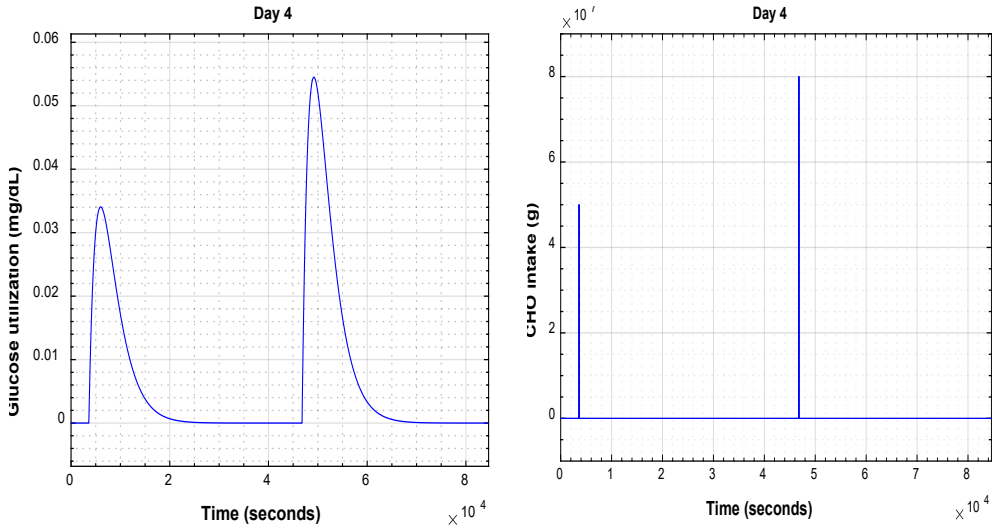

(a) (b)

Figure 6**.** Day 4. (**a**) Plot of glucose utilization against time (**b**) Plot of CHO intake against time

3. Results

This segment gives a comprehensive layout of the findings for the glucose-insulin dynamics in both open- and closed-loop scenarios throughout the four-day study. To understand the intricacies of blood glucose dynamics in the absence of corrective insulin infusion (open-loop scenario), a simulation with a constant zero control action was conducted. Furthermore, a closed-loop scenario was simulated using a fuzzy logic controller. The outcomes of these simulations are thoroughly examined in the subsequent subsections.

A. Open-loop Scenario: First Day

An in-depth exploration of the intricacies of the open-loop scenario was observed on the first day of the study. On the initial day, the individual's blood glucose exhibited variations of 100 mg/dl to 880 mg/dl, eventually converging to nearly 540 mg/dl. The attainment of a stable

glycemic state, as illustrated in Figure 7a, was not achieved, accompanied by the relevant insulin administration pace depicted in Figure 7b.

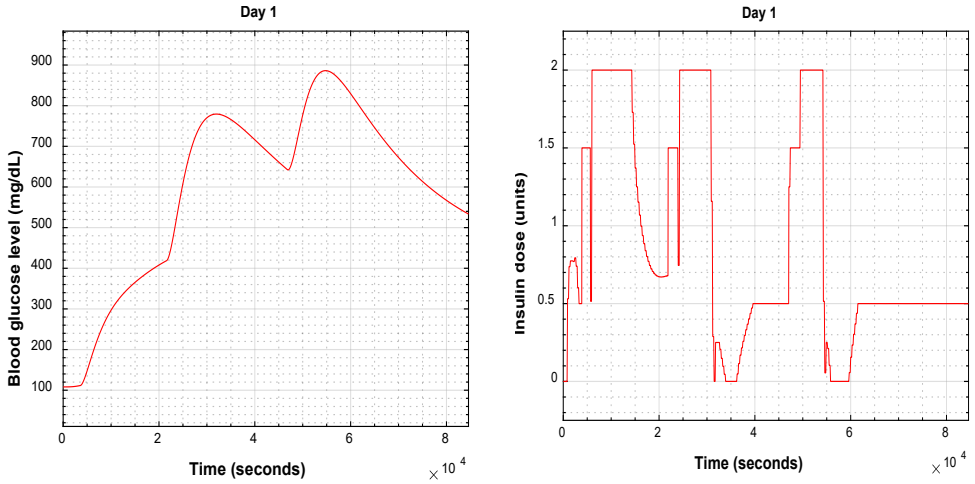

(a) (b)

Figure 7. Day 1. (a) Plot of blood glucose level against time
(b) Plot of insulin dose against time

A.1. Closed-loop scenario: first day

Figure 8a provides a visual representation of blood glucose levels, while Figure 8b illustrates the corresponding insulin injection patterns observed on the first day under the influence of an (FLC). In contrast, Figures 9a and 9b present a comparative analysis between the systems with and without tuning the membership function. The results demonstrated that with the introduction of the FLC, plasma glucose value around 108 and 195 mg/dl following glucose intake, ultimately settling at 80 mg/dl. Notably, a similar glycemic state was seen when the membership function was tuned.

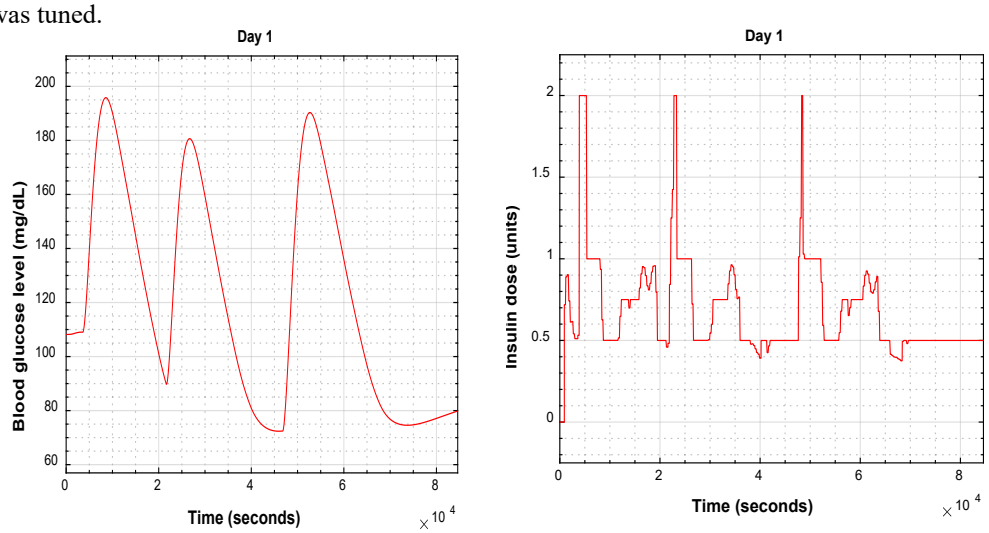

(a) **(b)**

Figure 8. Day 1. (**a**) Plot of Blood glucose level against time
(**b**) Plot of insulin dose against time.

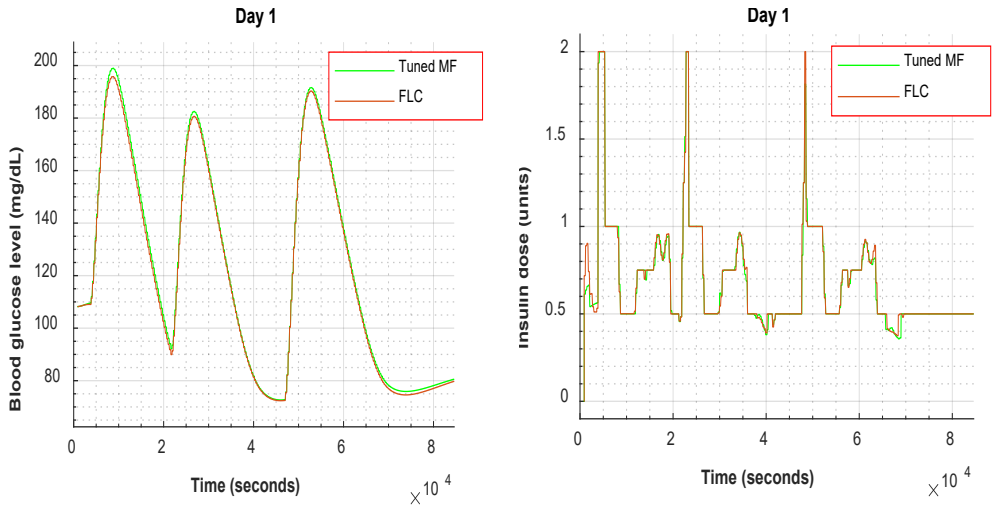

(a) (b)

Figure 9. Day 1. (**a**) Plot of blood glucose level against time considering tuned MF and FLC (**b**) Plot of insulin dose against time considering tuned MF and FLC.

B. Open-loop Scenario: Second Day

On the second day, the individual's blood glucose pace fluctuated between 103 mg/dl and 1000 mg/dl, eventually stabilizing at 550 mg/dl. The achievement of a stable glycemic state, as depicted in Figure 10a, was not realized with the associated insulin administration rate illustrated in Figure 10b.

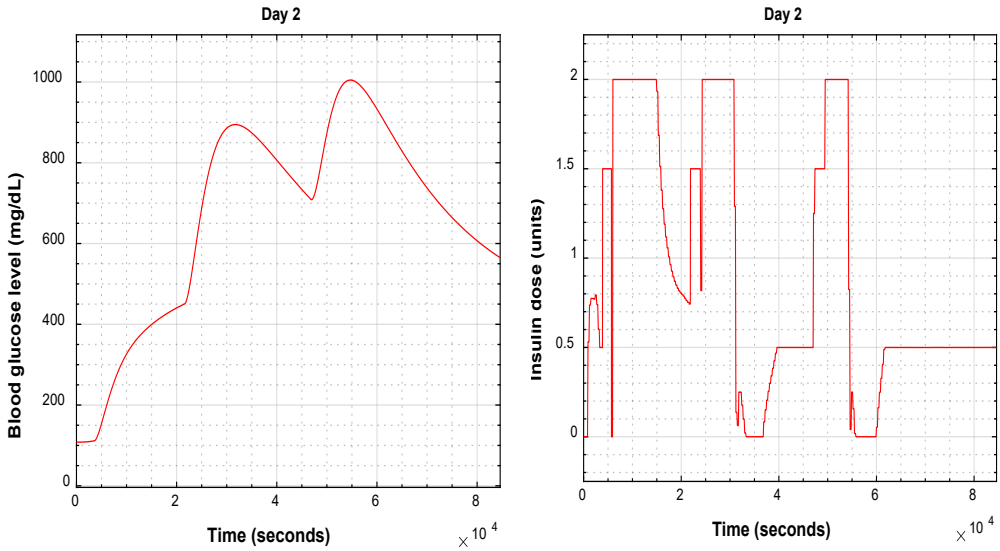

(a) (b)

Figure 10**.** Day 2. (**a**) Plot of blood glucose level against time (**b**) Plot of insulin dose against time.

B.1. Closed-loop scenario: Second day

The performance of the Fuzzy Logic Controller (FLC) on the second day is presented in Figure 11a (depicting blood glucose levels) and 11b (showing insulin injections). A comparative analysis of the system behavior with and without tuning the membership function is illustrated

in Figures 12a and 12b. Similar to the first day, the introduction of the control scheme resulted in plasma glucose level between 108 mg/dl and 215 mg/dl, eventually stabilizing at 80 mg/dl, indicating a significantly improved euglycemic state. Notably, a comparable glycemic state was achieved when the membership function was tuned.

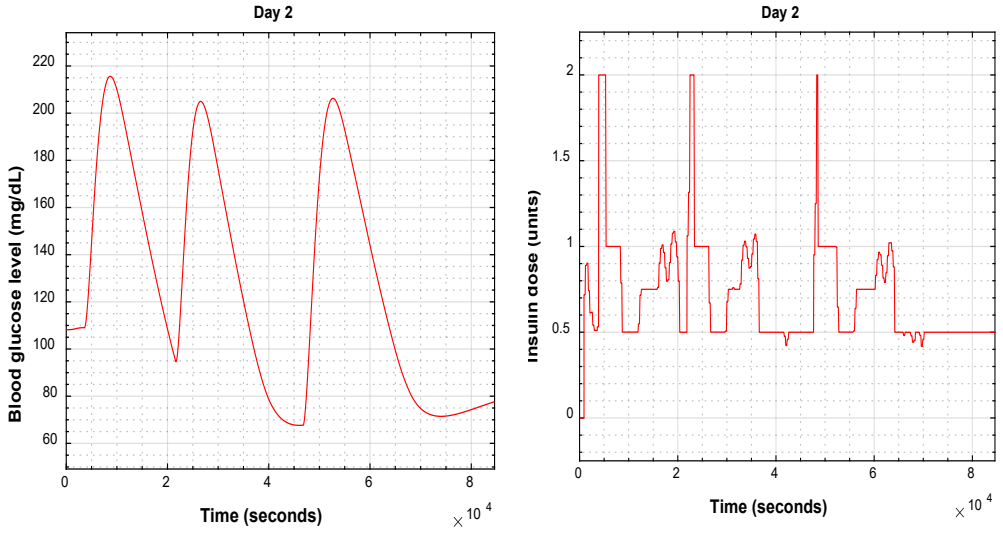

(a) (b)

Figure 11. Day 2. (**a**) Plot of blood glucose level against time (**b**) Plot of insulin dose against time.

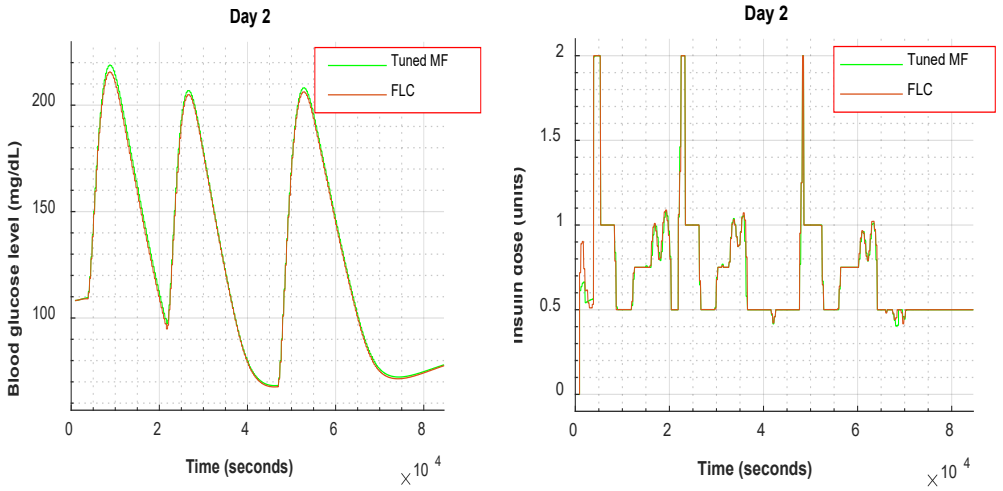

(a) (b)

Figure 12**.** Day 2. (**a**) Plot of blood glucose level against time considering tuned MF and FLC (**b**) Plot of insulin dose against time considering tuned MF and FLC.

C. Open-loop Scenario: Third Day

On the third day, the patient's blood glucose level exhibited fluctuations ranging from 108 mg/dl to 1000 mg/dl, ultimately stabilizing at 650 mg/dl. However, the attainment of a stable glycemic state, as depicted in Figure 13a, was not achieved along with the corresponding insulin administration pace shown in Figure 13b.

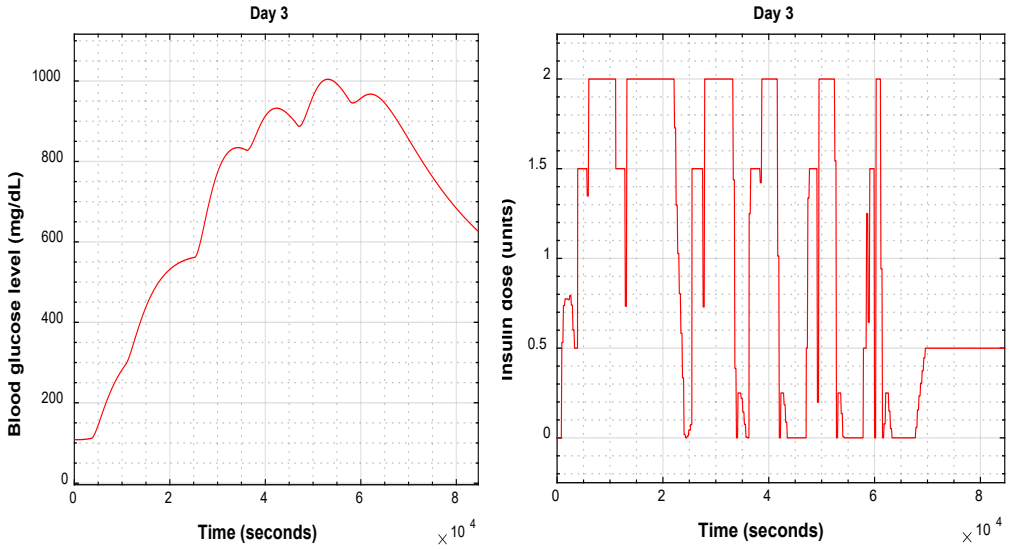

(**a**) (**b**)

Figure 13. Day 3. (**a**) Plot of blood glucose level against time (**b**) Plot of insulin dose against time.

C.1. Closed-loop Scenario: Third Day

The third-day performance of the Fuzzy Logic Controller (FLC) is shown in Figures 14a (representing blood glucose levels) and 14b (displaying insulin injections). A detailed comparative analysis of the system behavior with and without tuning the membership function is shown in Figures 15a and 15b. Consistent with the patterns observed in the preceding days, implementation of the control scheme led to plasma glucose level between 108 mg/dl and 190 mg/dl, eventually stabilizing at 80 mg/dl. This consistent outcome suggests a notable enhancement in the achievement of a euglycemic state. Importantly, a similar glycemic state was attained with the tuned membership function, emphasizing the robustness of the system under varying conditions.

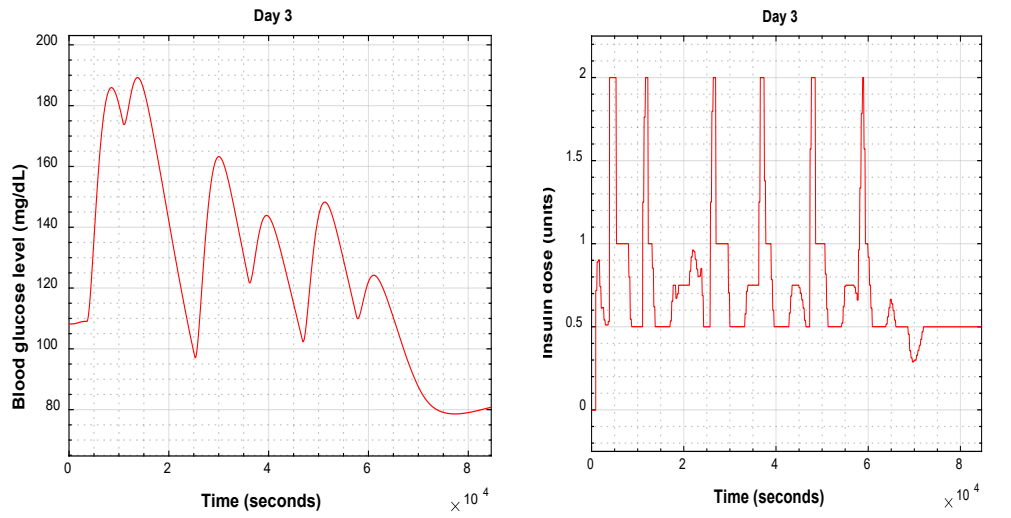

(**a**) (**b**)

Figure 14. Day 3. (**a**) Plot of blood glucose level against time (**b**) Plot of insulin dose against time.

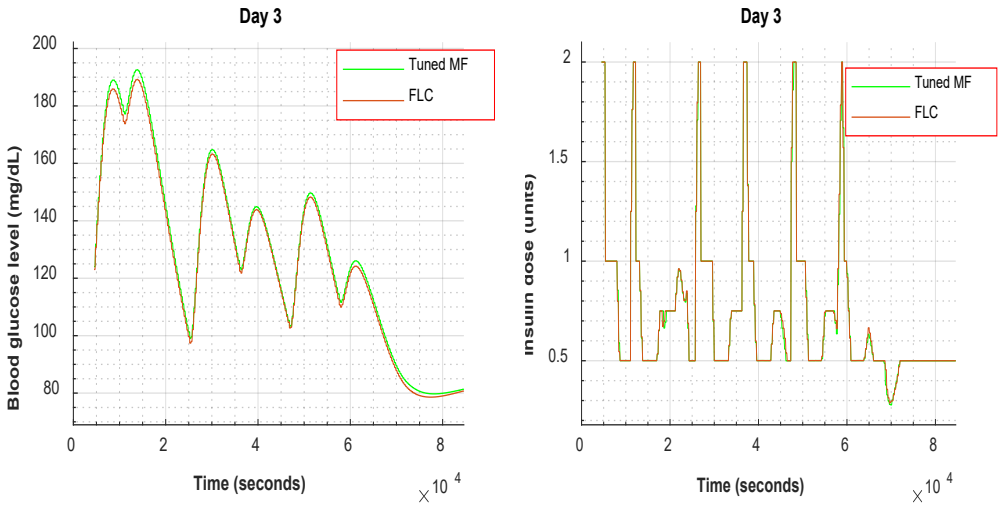

(**a**) (**b**)

Figure 15. Day 3. (a) Plot of blood glucose level against time considering tuned MF and FLC (b) Plot of insulin dose against time considering tuned MF and FLC.

D. Open-loop Scenario: Fourth Day

On the fourth day, blood glucose levels exhibited similar fluctuations to those observed in the previous days without corrective insulin infusion, ranging between 108 mg/dl and 830 mg/dl. The glycemic state eventually settled at approximately 520 mg/dl. However, similar to the other subjects, a stable glucose level was not attained, as illustrated in Figure 16a, along with the corresponding insulin infusion pace captured in Figure 16b.

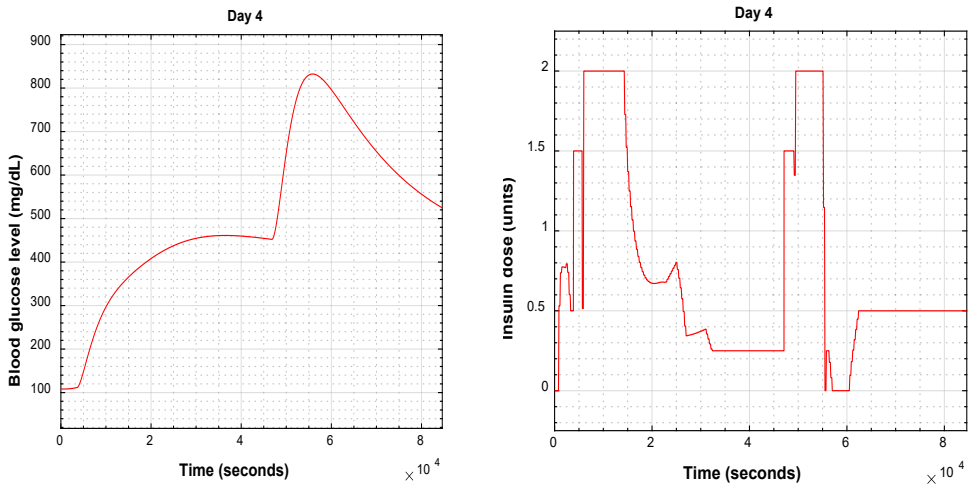

(**a**) (**b**)

Figure 16. Day 4. (**a**) Plot of blood glucose level against time (**b**) Plot of insulin dose against time.

D.1. Closed-loop Scenario: Fourth Day

Figure 17a provides a comprehensive visualization of blood glucose levels, whereas Figure 17b meticulously outlines the corresponding insulin injection patterns observed on the final day under the influence of the Fuzzy Logic Controller (FLC). Conversely, Figures 18a and 18b show

a detailed comparative analysis between systems with and without tuning the membership function. The results showed that with the integration of the FLC, the plasma glucose level between 108 and 238 mg/dl post-glucose intake, ultimately stabilizing at 75 mg/dl. This consistent outcome underscores a notable achievement in maintaining a desirable euglycemic state. Importantly, the tuned membership function demonstrated the ability to achieve a similar glycemic state, affirming the robustness of the control system under various conditions.

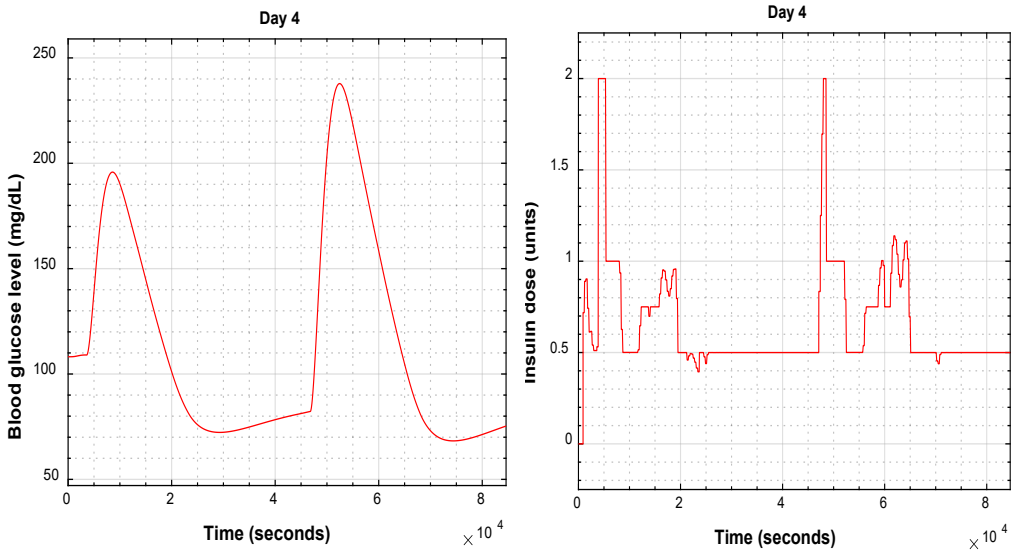

(**a**) (**b**)

Figure 17. Day 4. (**a**) Plot of blood glucose level against time
(**b**) Plot of insulin dose against time.

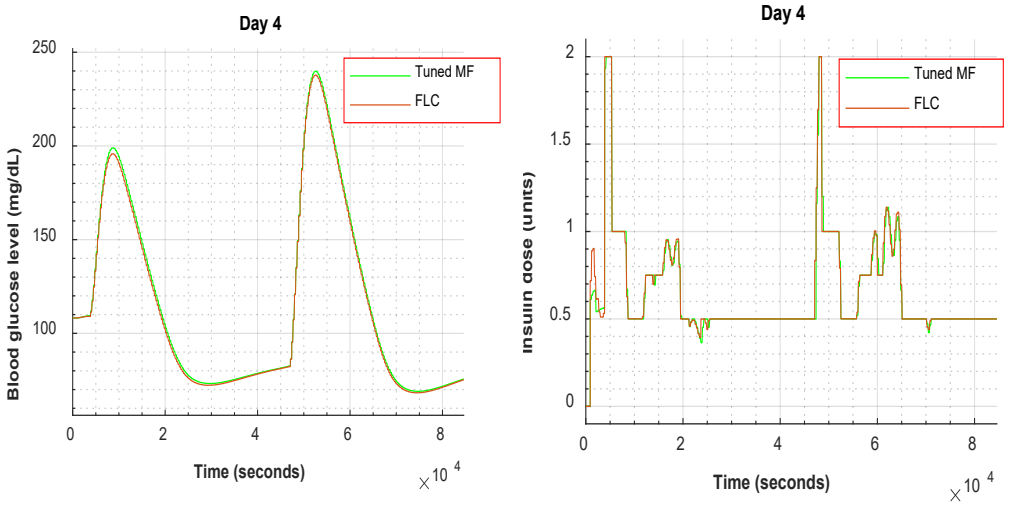

(**a**) (**b**)

Figure 18. Day 4. (**a**) Plot of blood glucose level against time considering tuned MF and FLC
(**b**) Plot of insulin dose against time considering tuned MF and FLC.

4. Evaluation metrics

To assess the efficacy of the control systems in monitoring BGL, globally recognized glycemic control parameters [32] were used for thorough assessments. Furthermore;

The evaluation of the system is presented in Table 6. Additionally, the Control Variability Grid Analysis (CVGA) for the postprandial meal was computed for four days, as depicted in Figures 19, 20, 21, and 22.

Table 6. Evaluation metrics for Hovorka's model in open and closed-loop systems over four days.

Day	Metrics	Open loop system	Closed-loop system
1	MG (mg/dl)	560	130.9
	TIR (%)	7.4	88.2
	> 180 (%)	92.6	11.8
	< 70 (%)	0	0
	< 54 (%)	0	0
	STD	254.6	50.9
	INS (U/day)	14.2	22.3
2	MG (mg/dl)	617.2	139.4
	TIR (%)	7.4	80.9
	> 180 (%)	92.6	16.2
	< 70 (%)	0	2.9
	< 54 (%)	0	0
	STD	297.3	60.8
	INS (U/day)	13.2	22.7
3	MG (mg/dl)	685.3	134.8
	TIR (%)	7.4	94.2
	> 180 (%)	92.6	5.8
	< 70 (%)	0	0
	< 54 (%)	0	0
	STD	355.7	34.3
	INS (U/day)	27.4	31.6
4	MG (mg/dl)	467.6	137.2
	TIR (%)	5.8	92.6
	> 180 (%)	94.2	7.4
	< 70 (%)	0	0
	< 54 (%)	0	0
	STD	230.3	67
	INS (U/day)	11.1	20.2

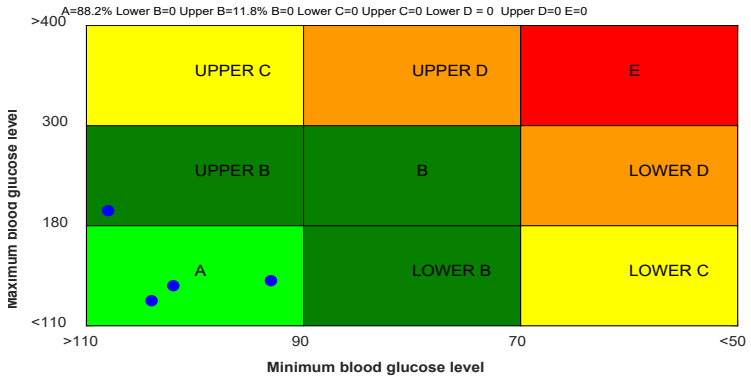

Figure 19. CVGA of day 1.

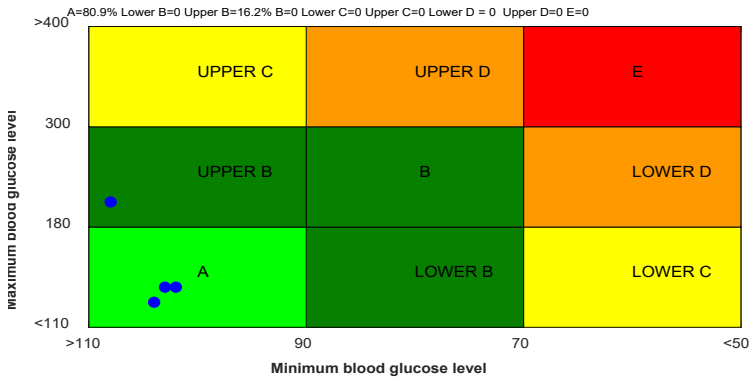

Figure 20. CVGA of day 2.

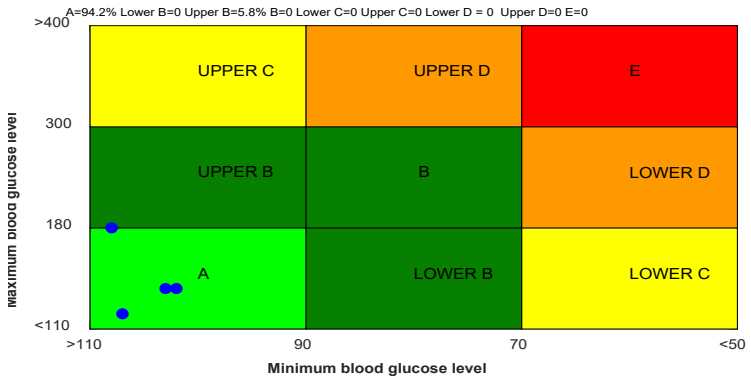

Figure 21. CVGA of day 3.

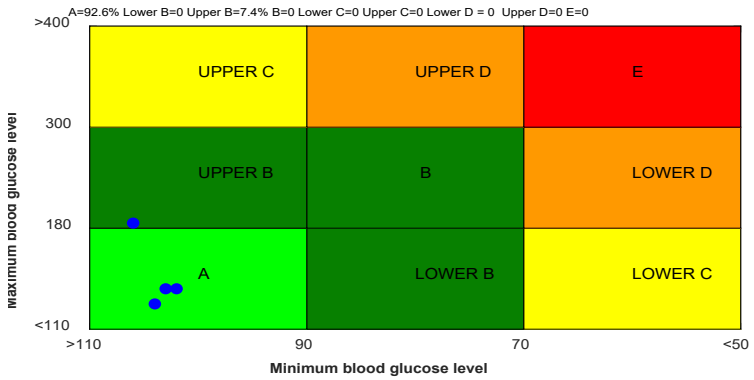

Figure 22. CVGA of day 4.

5. Discussion and Conclusions

The controller showed satisfactory performance during the first day, effectively adapting to variations in insulin sensitivity under normal dietary conditions. On the second day, when confronted with substantial meals, the closed-loop system demonstrated noteworthy performance by preventing excessive insulin injections through optimization of membership function parameters. Throughout the third day, the controller consistently maintained an acceptable performance, as evidenced by the mean blood glucose levels, even when faced with an additional meal protocol. However, under the conditions of reduced meals on the fourth day, the proposed system exhibited robustness. It should be noted that optimal functionality in this scenario necessitates an increased frequency of insulin injections. Conclusively, in this study, an

in-depth exploration of the open- and closed-loop systems utilizing Hovorka's model for glucose-insulin kinetics, reflecting the physiological aspects of diabetic individuals, was conducted over four days. The examination revealed a noteworthy decrease in the standard deviation, representing the variability of blood glucose levels from their mean, in the closed-loop system employing the fuzzy-logic controller compared to its open-loop counterpart. This reduction suggests an optimal health status for individuals under closed-loop control. While this study focused primarily on the biological state of investigating glucose kinetics, it is imperative to acknowledge that patient glycemic significance could be further emphasized through alternative strategies, such as data-driven approaches, and the current research exclusively considered the meal model as an external disturbance. However, future investigations could encompass alternative mathematical models incorporating factors such as stress, sleep, and physical activities. Understanding and incorporating these elements would contribute to a more adaptive and comprehensive model for managing blood glucose concentrations in patients with diabetes.

6. Acknowledgment

The authors express their gratitude for the support received from UEMF and ASRIC-AU.

7. References

[1] M. Wysocka-Mincewicz, E. Szczerbik, M. Mazur, M. Grabik, M. Kalinowska, and M. Syczewska, "Foot Plantar Pressure Abnormalities in Near Adulthood Patients with Type 1 Diabetes," *Biomedicines,* vol. 11, no. 11, p. 2901, 2023. [Online]. Available: https://www.mdpi.com/2227-9059/11/11/2901.

[2] M. S. Popoviciu, N. Kaka, Y. Sethi, N. Patel, H. Chopra, and S. Cavalu, "Type 1 Diabetes Mellitus and Autoimmune Diseases: A Critical Review of the Association and the Application of Personalized Medicine," *Journal of Personalized Medicine,* vol. 13, no. 3, p. 422, 2023. [Online]. Available: https://www.mdpi.com/2075-4426/13/3/422.

[3] S. A. Antar *et al.*, "Diabetes mellitus: Classification, mediators, and complications; A gate to identify potential targets for the development of new effective treatments," *Biomedicine & Pharmacotherapy,* vol. 168, p. 115734, 2023.

[4] A. Singh *et al.*, "Recent trends and advances in type 1 diabetes therapeutics: A comprehensive review," *European Journal of Cell Biology,* p. 151329, 2023.

[5] I. N. Abubakar, M. Essabbar, and H. Saikouk, "Analysis of the performances of various controllers adopted in the biomedical field for blood glucose regulation: a case study of the type-1 diabetes," *Journal of Medical Engineering & Technology,* pp. 1-13, 2024.

[6] I. N. Abubakar, M. Essabbar, and H. Saikouk, "Optimizing Blood Glucose Regulation in Type 1 Diabetes Patients via Genetic Algorithm-Based Fuzzy Logic Controller Considering Substantial Meal Protocol," 2024.

[7] A. I. Ndakara, M. Essabbar, and H. Saikouk, "Blood Glucose-Insulin Dynamics in Type-1 Diabetic Patients for the Mitigation of Hyperglycemic Conditions: A PID Controller with a Step Response," in *Digital Technologies and Applications: Proceedings of ICDTA'23, Fez, Morocco, Volume 1*: Springer, 2023, pp. 949-956.

[8] M. S. Ali *et al.*, "Diabetes Mellitus Control Including Fruits in Diet: Exhaustive Review and Meta-analysis," *Asian Journal of Food Research and Nutrition,* vol. 3, no. 1, pp. 43-59, 2024.

[9] M. Qaraqe, A. Elzein, S. Belhaouari, M. S. Ilam, and G. Petrovski, "A novel few shot learning derived architecture for long-term HbA1c prediction," *Scientific Reports,* vol. 14, no. 1, p. 482, 2024.

[10] J. Ding *et al.*, "Association of HbA1c Variability with Vibrating Perception Threshold in Middle-Aged and Elderly Patients with Type 2 Diabetes Mellitus: A Retrospective Cohort Study," *Diabetes, Metabolic Syndrome and Obesity,* pp. 193-202, 2024.

[11] A. D. G.-M. Vásquez and J. J. M. Rodríguez, "Quality of Life in Adult Patients with Diabetes," in *The Role of Nutrition in Integral Health and Quality of Life*: Apple Academic Press, 2024, pp. 495-506.

[12] T. F. Roohi *et al.*, "Beyond drug discovery: Exploring the physiological and methodological dimensions of zebrafish in diabetes research," *Experimental Physiology,* 2024.
[13] B. Lalani, K. Gosselin, R. Penno, B. Puryear, H. Rilo, and A. Lalani, "A Retrospective Cohort Analysis of Two Computerized Insulin Infusion Protocols," *Journal of Diabetes Science and Technology,* vol. 17, no. 3, pp. 635-641, 2023.
[14] L. Liu, Z. Liu, B. Duan, Q. Zhang, Z. Zhou, and W. Liu, "Effects of a low glycemic index or low glycemic load diet on pregnant women at high risk of gestational diabetes: A meta-analysis of randomized controlled trials," *Nutrition, Metabolism and Cardiovascular Diseases,* vol. 33, no. 10, pp. 2006-2018, 2023.
[15] Y. R. Kim, M. J. Park, S.-y. Park, and J. Y. Kim, "Brown Seaweed Consumption as a Promising Strategy for Blood Glucose Management: A Comprehensive Meta-Analysis," *Nutrients,* vol. 15, no. 23, p. 4987, 2023. [Online]. Available: https://www.mdpi.com/2072-6643/15/23/4987.
[16] S. Kraithong, A. Theppawong, N. Bunyameen, X. Zhang, and R. Huang, "Advancements in understanding low starch hydrolysis in pigmented rice: A comprehensive overview of mechanisms," *Food Chemistry,* p. 138079, 2023.
[17] I. S. Parida, S. Takasu, and K. Nakagawa, "A comprehensive review on the production, pharmacokinetics and health benefits of mulberry leaf iminosugars: main focus on 1-deoxynojirimycin, d-fagomine, and 2-O-α-d-galactopyranosyl-DNJ," *Critical Reviews in Food Science and Nutrition,* vol. 63, no. 19, pp. 3468-3496, 2023.
[18] M. G. Nuzzo and M. Schettino, "Advanced Technology (Continuous Glucose Monitoring and Advanced Hybrid Closed-Loop Systems) in Diabetes from the Perspective of Gender Differences," *Diabetology,* vol. 4, no. 4, pp. 519-526, 2023. [Online]. Available: https://www.mdpi.com/2673-4540/4/4/45.
[19] E. Zhang *et al.*, "An injectable and biodegradable zwitterionic gel for extending the longevity and performance of insulin infusion catheters," *Nature Biomedical Engineering,* pp. 1-17, 2023.
[20] S. Mandal and A. Sutradhar, "Robust controller for artificial pancreas for patients with type-1 diabetes," *Research on Biomedical Engineering,* pp. 1-14, 2023.
[21] S. Khodakaramzadeh, Y. Batmani, and N. Meskin, "Automatic blood glucose control for type 1 diabetes: A trade-off between postprandial hyperglycemia and hypoglycemia," *Biomedical Signal Processing and Control,* vol. 54, p. 101603, 2019/09/01/ 2019, doi: https://doi.org/10.1016/j.bspc.2019.101603.
[22] A. Sharma, Nilam, and H. P. Singh, "Computer-controlled diabetes disease diagnosis technique based on fuzzy inference structure for insulin-dependent patients," *Applied Intelligence,* vol. 53, no. 2, pp. 1945-1958, 2023.
[23] A. Sayed, B. A. Zalam, M. Elhoushy, and E. Nabil, "Optimized type-2 fuzzy controller based on IoMT for stabilizing the glucose level in type-1 diabetic patients," *Scientific Reports,* vol. 13, no. 1, p. 14508, 2023.
[24] M. Elhoushy, B. A. Zalam, A. Sayed, and E. Nabil, "Automated blood glucose regulation for nonlinear model of type-1 diabetic patient under uncertainties: GWOCS type-2 fuzzy approach," *Biomedical Engineering Letters,* pp. 1-25, 2023.
[25] R. Hovorka *et al.*, "Nonlinear model predictive control of glucose concentration in subjects with type 1 diabetes," (in eng), *Physiol Meas,* vol. 25, no. 4, pp. 905-20, Aug 2004, doi: 10.1088/0967-3334/25/4/010.
[26] M. E. Wilinska, L. J. Chassin, H. C. Schaller, L. Schaupp, T. R. Pieber, and R. Hovorka, "Insulin kinetics in type-1 diabetes: continuous and bolus delivery of rapid acting insulin," *IEEE Transactions on Biomedical Engineering,* vol. 52, no. 1, pp. 3-12, 2004.
[27] T. Peyser, E. Dassau, M. Breton, and J. S. Skyler, "The artificial pancreas: current status and future prospects in the management of diabetes," *Annals of the New York Academy of Sciences,* vol. 1311, no. 1, pp. 102-123, 2014.

[28] M. Breton and B. Kovatchev, "Analysis, modeling, and simulation of the accuracy of continuous glucose sensors," *Journal of diabetes science and technology,* vol. 2, no. 5, pp. 853-862, 2008.
[29] L. Magni *et al.*, "Model predictive control of type 1 diabetes: an in silico trial," ed: SAGE Publications, 2007.
[30] C. Dalla Man, R. A. Rizza, and C. Cobelli, "Meal simulation model of the glucose-insulin system," *IEEE Transactions on biomedical engineering,* vol. 54, no. 10, pp. 1740-1749, 2007.
[31] B. P. Kovatchev, M. Breton, C. Dalla Man, and C. Cobelli, "In silico preclinical trials: a proof of concept in closed-loop control of type 1 diabetes," ed: SAGE Publications Sage CA: Los Angeles, CA, 2009.
[32] D. M. Maahs *et al.*, "Outcome measures for artificial pancreas clinical trials: a consensus report," *Diabetes care,* vol. 39, no. 7, pp. 1175-1179, 2016.

Isah Ndakara Abubakar is a PhD student at the Euro Mediterranean University of Fes, UEMF, Morocco. His research interests include electronics, power, control systems, sensors, and data acquisition in the biomedical field.

Moad Essabbar holds a Ph.D. in Engineering, and he is currently an Associate Professor at the Euromed University of Fes, UEMF, Morocco. His research areas include electronics, sensors, and embedded systems.

Hajar Saikouk holds an engineering degree in Mechatronics from ENSA Fez (2014) and a Ph.D. in Electronics from the University of Montpellier, France (2018). She completed a postdoctoral fellowship at Sherbrooke University, Canada. She was an Assistant Professor at Euromed University of Fes (UEMF) from 2020 to 2024, and joined Mohammed V University of Rabat as an Assistant Professor in 2024. Her research focuses on electronics, sensors, ultrasound, and data acquisition, with applications in medicine and agriculture.

El Hilali Alaoui Ahmed is a prominent mathematician with a robust background in mathematical sciences and optimization. He completed his B.Sc. in Mathematical Sciences at Tarik Ibn Ziad High School in 1978 and pursued higher education at Mohammed V University in Rabat, earning a DEUG in Mathematics and Physics in 1980 and a degree in Applied Mathematics in 1982. Ahmed further specialized in analysis and optimization, obtaining a CEUS in 1986, a DUES in 1989, and a State Doctorate in 1996 from Sidi Mohamed Ben Abdellah University in Tetouan. He is currently a professor at the EIDIA department of the Euromed University of Fes, UEMF, Morocco.